Novel polyethylene terephthalate (PET) plastic degrading enzymes from the environmental metagenome

Isuru Karunatillaka[1], Lukasz Jaroszewski[2] and Adam Godzik[2]*

[1] Undergraduate Research Project, College of Natural and Agricultural Sciences, University of California Riverside, 900 University Ave., Riverside, CA, 92521, USA

[2] Biosciences Division, University of California Riverside School of Medicine, 900 University Ave., Riverside, CA, 92521, USA

* Corresponding author
E.mail: adam.godzik@medsch.ucr.edu

Abstract

Several plastic degrading enzymes have been described in the literature, most notably PETases that are capable of hydrolyzing polyethylene terephthalate (PET) plastic. One of them, the PETase from *Ideonella sakaiensis*, a bacterium isolated from environmental samples within a PET bottle recycling site, was the subject of extensive studies. To test how widespread PETase functionality is in other bacterial communities, we used a cascade of BLAST searches in the JGI metagenomic datasets and showed that PETases can also be found in other metagenomic environmental samples from both human affected and relatively pristine sites. To confirm their classification as PETases, we verified that the newly identified proteins have the PETase sequence signatures common to all PETases and that phylogenetic analyses group them with the experimentally characterized PETases. Additionally, docking analysis was performed in order to further confirm the functional assignment of the putative environmental PETases.

Introduction

Polyethylene terephthalate (PET) plastic is one of the most widely used plastic materials for consumer products and packaging [1]. The widespread use of PET has resulted in its harmful accumulation in the environment, endangering wildlife and human health alike. With the recycling rate of PET bottles and jars being only 29.1% in 2017, there is a large commercial interest in looking for more efficient means of biological recycling in order to increase PET recycling rates [2].

PETases are an esterase class of enzymes which catalyze the hydrolysis of PET into mono-2-hydroxyethyl terephthalate (MHET), with minor amounts of terephthalic acid (TPA) and bis(2-hydroxyethyl) TPA (BHET). These enzymes can further hydrolyze BHET into MHET with no further hydrolysis [3]. PETases are a subset of a broader protein family of cutinases, enzymes that hydrolase cutin, which is one of two waxy polymers that are the main components of the cuticle that covers all aerial surfaces of plants. Despite their close homology, PETases can be distinguished from classical cutinases by the presence of specific sequence motifs and by phylogeny, which will be elaborated upon further in this paper.

The first discovered PETase came from the bacteria *Ideonella sakaiensis* strain 201-F6, which was cloned from the environmental samples taken from a PET bottle recycling site in Sakai, Osaka Prefecture [4]. After the sequencing of its genome, the enzyme responsible for the PETase activity was identified as a product of the gene ISF6_4831 and was shown to be capable of degrading PET film of roughly 15% crystallinity (commercial soft drink bottles typically have PET crystallinity of 15.7% at pH 7.2 [5]). The *I. sakaiensis* PETase has a PET film degradation rate of 0.13 mg cm^{-2} day^{-1} at 30℃ [4]. Its structure was later determined by X-ray crystallography and deposited into the Protein Data Bank (PDB) with the code 6EQD.

Aside from the *I. sakaiensis* PETase, at least 69 PETase-like enzymes from a variety of terrestrial and aquatic soil bacteria are currently known, however the *I. sakaiensis* enzyme remains the most efficient [3].

Despite its relatively high efficiency, the *I. sakaiensis* PETase is still far too slow for industrial scale PET plastic recycling. Since an industrialized biological recycling of PET plastic would have a much lower cost than current PET plastic recycling methods, eliminating roadblocks to scalability is paramount. Eliminations of such roadblocks can occur by either finding ways to improve the efficiency of the *I. sakaiensis* PETase or finding new, more efficient, PETases.

PETases have conserved Ser-His-Asp catalytic triads indicating catalytic mechanisms shared with other esterases [3, 6]. Additionally, two binding subsites and a stabilizing disulfide bridge within the binding site were identified as being specific to PETases. Known PETases were classified into three types (type I, IIa, and IIb). PETases of type IIb are the most efficient and *I. sakaiensis* PETase belongs to this group [3].

The two subsites of PETases work cooperatively with the catalytic triad to initially conduct a nick generation step which breaks the PET into two chains, one with a TPA-terminal released from subsite I and another with a HE-terminal released from subsite II. A terminal digestion step then occurs, which varies in outcome depending on the configurations of these two chains within the binding site. The predominant products that accumulate from this final step are MHET, TPA, and ethylene glycol [3]. These compounds can then be utilized by the bacterial organism for growth. Importantly, they can also be used to create new plastics or numerous other polyester consumer products. PETases could serve as a major solution to plastic pollution in both terrestrial and aquatic habitats [7].

Figure 1 goes here.

In this publication, we assume that the conservation of the residues that constitute the catalytic triad, the two subsites, and the disulfide bridge of all known PETases can be used in combination with a cascade of sequence-based homology searches to identify candidates for novel PETases and, relying on this assumption, identify candidate PETases in the Joint Genome Institute (JGI) terrestrial metagenome microbiome samples [8]. We show that PETases are widely distributed in different environments and suggest that systematic searches for new PETases in the environmental metagenomes may yield many novel PETases.

Results

Putative PETases found in environmental samples

Using the search strategy described in detail in the Methods section, we identified 27 putative PETases (further denoted PETen1-27) from 24 environmental metagenomics samples in the JGI Integrated Microbial Genomes & Microbiomes (IMG/M) resource [8]. All of the candidate PETases (see the full list included in supplementary table S1) share identical or similar residues, with few exceptions, in positions constituting the catalytic site, subsite I, and subsite II, in all currently known PETases/PETase-like enzymes. Since these putative PETases come from metagenomic sequencing projects, many of the sequences were incomplete and did not include some of the aforementioned functionally important residues. Here we focused on two candidate PETases (PETen1 and PETen2) whose sequences are sufficiently complete to include all of their functionally important motifs (see Table 1).

Table 1 goes here

Our data shows conservation of many significant residues in globally distributed environmental metagenomic proteins which match the residues/ positions in the catalytic triad, subsite I, subsite II, and additional disulfide bond of *I. sakaiensis* PETase. Examination of PETen1 and 2 specifically shows that most of the binding site residues are conserved. In PETen1, the only substitution is from polar T88 to nonpolar L88, while PETen2, has Y87F, A89E, and W159H substitutions. It has been shown by Joo et. al. [3] that in PETases, W159H variants have decreased PET-degrading activity, but site-directed mutagenesis of T88L, Y87F, nor A89E variants have not been reported. The other binding site residues of importance which are critical for defining efficient type IIb PETases are present in the metagenomic PETases, including the catalytic triad and an additional disulfide bridge (C203 and C239). The disulfide bond is indicative of a structure conformation which keeps H237 engaged in the catalytic triad, holding together subsite II, and improving thermal stability. This disulfide bridge, which so far has been unique to *I. sakaiensis* PETase and other type II PETases, is found within both PETen1 and 2. Joo et. al. emphasizes the importance of an extended loop constituting positions S242, G243, N244, S245, N246, Q247 for holding together subsite II and the catalytic triad. This extended loop, which is also unique to *I. sakaiensis* PETase and other type II PETases, is conserved within PETen1 and 2 (an exception being Q247). Additionally, PETen1 is unique in that it has a natural R280A mutation, which has been shown to improve the catalytic rate in *I. sakaiensis* PETase mutants over the wildtype by 22.4% in 18 hours and 32.4% in 36 hours [1 9]. The fact that the majority of the binding site

residues in PETen1 and 2 match those indicative of type IIb PETases, strongly suggests that they are type IIb putative PETases.

In regard to the other collected putative PETases, PETen 1, 2, 17, 18, and 20 contain all of the motif residue positions of each binding site feature and seem to be full length sequences (see supplementary table S1). In PETen 17 all the functionally important residues are fully conserved with *I. sakaiensis* PETase. In PETen 3, 8, 10, 12, 14, 15, 16, 19, 21, 23, and 24 most of the functional motif residue positions are conserved.

Verification of the putative PETases by modeling and docking calculations

Homology modeling and docking were performed to further examine the validity of classifying both proteins as putative PETases rather than classical cutinases. To accomplish this, tertiary structures of both proteins were predicted using Robetta [10] and docking experiments were performed using AutoDock Vina [11]. The predicted structures of both PETen1 and 2 have significant structural similarity to *I. sakaiensis* PETase with both having a p-value <0.01. It is noteworthy that these sequences are homologous to *I. sakaiensis* PETase, and therefore it is expected that the structure prediction software would produce structures that are similar to the *I. sakaiensis* PETase. Therefore, the predicted structures may be different from their true structures and the docking results should be considered with caution until experimental structures are available.

Table 2 goes here

As shown by the docking results (see Table 2), PETen1, PETen2, and *I. sakaiensis* PETase had similar and consistently lower (more favorable) binding energies for PET compared to the classical cutinase *Fusarium solani* f. sp. *pisi* [12]. Additionally, the classical cutinase had a lower binding energy for cutin than either PETen1, PETen2 or *I. sakaiensis* PETase.

Surprisingly, the *Fusarium solani* f. sp. *pisi* cutinase did not show as strong of a preference for the cutin molecule as might be expected. This could be due to the oligo-polyester differing from the actual cutin substrate that the enzyme naturally degrades, especially considering the vast range of different existing cutin polymers. It should also be noted that the orientations of the docked 2-HE$(MHET)_4$ in relation to PETen1 and 2 were very similar to its docked orientation in *I. sakaiensis* PETase (Figure 1) due to their unobstructed binding site clefts. On the other hand, the *Fusarium solani* f. sp. *pisi* binding site cleft is not continuous - in a very similar fashion to *Tf*Cut2 in Figure 5 of Joo et. al.[1] - therefore the shortened PET molecule docked in an unrealistically convoluted manner. Due to the binding preference and the more realistic docking conformations that the two metagenomic proteins and *I. sakaiensis* PETase have with PET, these data support the classification of PETen1 and PETen2 as putative PETases rather than classical cutinases.

Weblogo Comparison

In order to further compare the metagenomic PETases, experimentally verified PETases and cutinases, we prepared weblogos[13] representing key functional residues (Figure 2).

Figure 2 goes here

The Weblogos show that for subsite I, Q119, M161 and W185 are conserved in the metagenomic PETases as well as known PETases, while Y87 is commonly replaced with phenylalanine in both groups. For subsite II positions, polar T88 is frequently replaced by nonpolar L88 in metagenomic PETases and in known PETases. Nonpolar A89 is not as conserved as the other binding site residues and is replaced by acidic glutamate in a small percentage of metagenomic sequences. The W159 residue (adjacent to the serine

nucleophile) is commonly replaced with histidine in both the metagenomic and previously known PETases. Polar S238 and N241 are strongly conserved in the metagenomic PETases. The catalytic triad (S160, D206, and H237) is conserved within all the metagenomic PETases.

Comparison of the Weblogos shows that, overall, the new metagenomic sequences have a high abundance of binding site residues conserved with the *I. sakaiensis* PETase binding site residues. S238 found in *I. sakaiensis* PETase is much more dominant in the metagenomic proteins than the previously determined PETases. S238, along with W159, plays a crucial role in higher PET-degrading ability by making the binding cleft more shallow, thereby making the catalytic site more accessible [3]. Also, T88 and A89 in I. *sakaiensis* have higher conservation in the metagenomic proteins than the previously determined PETases.

The critical additional disulfide bridge residues (C203 and C239), are found in all of the metagenomic PETases with sufficiently complete sequences confirming likelihood of PET degradation ability.

Additionally, PETens 1, 2, 8b, 14, 15a, and 22 of the metagenomic sequences contain an extended loop (N244, S245, N246) which is important for maintaining a continuous binding cleft [1]. This extended loop is exclusive to only *I. sakaiensis* PETase and other type II PETases. Upon examination of the cutinase weblogo [13], it is apparent that the metagenomic PETases do not match the binding site positions of cutinases. Several residues such as S87, Y159, Q161, T185 are conserved in cutinases but are not present in corresponding positions of the metagenomic PETases nor previously determined PETases. This confirms that the metagenomic sequences collected in this study are indeed PETases and not cutinases.

The sequences of the putative PETases were checked by reciprocal BLAST [14] in the NCBI NR datatase and for all of them the *I. sakaiensis* PETase or one of the other annotated type II PETases were the top BLAST hits.

Phylogenetic Analysis

In order to further verify that the selected metagenomic sequences represent PETases, a phylogenetic tree was prepared (for details, see Methods section). All PETases marked by stars in Figure 3 were identified by Joo et. al. [1]. The representative group of classical cutinases are non-hypothetical and were taken at random from Uniprot (full sequences found in supplementary table S4), none of which have documented PET degrading ability [15].

Figure 3 goes here

As can be seen in the phylogenetic tree, previously determined PETases of all types - along with the metagenomic sequences - form a separate branch of considerable length away from classical cutinases. The classical cutinase branch has a bootstrap value of 100%. This indicates that none of the metagenomic sequences should be considered just regular cutinases. Metagenomic PETen 4 can be considered a putative type I PETase based on our phylogenetic tree and the sequence motif of type I PETases by Joo et. al. There are no PETens which correlate phylogenetically to type IIa PETases. However, every other PETen phylogenetically fits with type IIb PETases in a common clade, reinforcing our aforementioned classification of PETen1 and 2 as putative type IIb PETases. Our tree shows that the metagenomic sequences of closest homology to *I. sakaiensis* PETase come from proteins 14, 22, and 15a. PETen1 shares more sequence homology to the PETase from

Burkholderiales bacterium RIFCSPLOWO2 and PETen 2 shares more sequence homology to the PETase from *Polyangium brachysporum*.

Discussion

In this work we have identified 27 putative PETases, from which we have used two (PETen1 and PETen2) to further argue for their classification as PETases through sequence and docking analysis. Additionally, we have shown how the new metagenomic sequences are highly similar to known PETases by comparative Weblogos and phylogenetic analysis.

Surprisingly, in contrast to the *I. sakaiensis* PETase, which was discovered in a plastic recycling center, nearly all of the proposed metagenomic PETases were taken from areas that are relatively pristine and probably free from substantial plastic pollution. This indicates that the selection that led to the emergence of PETase activity may have been in response to a natural polymer, possibly a cutin variant, with similar molecular structure to PET polymers. As our data suggests, PETases may have branched independently from classical cutinases much earlier than previously thought and, most likely, without the specific impact of human-made PET polymers. With no notable commonalities between the samples' environments, this raises the question of what specific environmental substrate led to PETases branching off from classical cutinases if not some variant of cutin?

It is noteworthy that our searches only included the terrestrial JGI microbiome metagenomes (7,375 samples). We did not perform searches in aquatic, airborne, engineered, host-associated, and undetermined origin metagenomic samples which constitute a total of 28,112 samples. Additional limitations of our data include the previously mentioned use of structure prediction for the two full length sequences. Since the sequences are homologous to the *I. sakaiensis* PETase, it is expected that the predicted

structures would be similar to *I. sakaiensis* PETase, therefore the docking analysis should be considered with caution.

Overall, we have demonstrated that there are a significant number of previously uncharacterized proteins in the metagenomes that can be reliably predicted to have the capability of PET degradation. Before this publication, 69 possible PETases were known, all from known organisms; our work suggests that the number of PETases could be expanded by systematic analysis of metagenomic samples. The future steps would include crystallization of the full-length putative type IIb PETases, including the two analyzed in this paper, in order to more reliably assess their PET-degrading capabilities.

Materials and Methods

Data Collection

Metagenomic sequences were obtained by conducting BLAST searches on 7,375 terrestrial metagenomic samples in the JGI Integrated Microbial Genomes and Microbiomes database [8] with *I. sakaiensis* PETase used as the query. Only proteins with ≥60% sequence identity to *I. sakaiensis* PETase were considered for further analysis. Sequences of these 27 proteins were then checked by reciprocal BLAST (each PETen used as a query) in the NCBI NR database in order to make sure their top BLAST hit is the *I. sakaiensis* PETase or another type IIb PETase. The sequences were manually analyzed for the presence of the various sequence motifs (see Figure 2). PETen2 has an extra N-terminal region which appears to be an artifact of the metagenomic sequencing, as no known PETase or cutinase contains a homologous region [16]. This extra N-terminal region which extends to Gly178 was consequently removed from the sequence used in our analysis.

Structure Prediction and Docking

The structures for the two selected putative PETases (PETen1 and PETen2) were predicted by using Robetta [10]. FATCAT was then used in order to verify that the structures are similar to *I. sakaiensis* PETase as expected [17]. The docking binding energies of the two metagenomic proteins, *I. sakaiensis* PETase, and the cutinase from *Fusarium solani pisi* were generated using Autodock Vina [11] as part of UCSF Chimera [18].

Weblogo

The weblogos were made using Berkeley Weblogo 2.8.2 [13] after aligning the sequences using MUSCLE [19]. The sequences were trimmed to only include the residues of interest in the weblogos.

Phylogenetic Tree

In order to construct the phylogenetic tree, the web server IQ-TREE [20] was used to generate the maximum likelihood tree with 50% of gaps removed from the MUSCLE multiple alignment [19]. The tree was then visualized using iTol Tree of Life v5.0 [21].

References

1. Andrady, A.L. and M.A. Neal, *Applications and societal benefits of plastics*. Philos Trans R Soc Lond B Biol Sci, 2009. **364**(1526): p. 1977-84.
2. EPA, E.P.A. *Plastics: Material-Specific Data*. 2020; Available from: www.epa.gov/facts-and-figures-about-materials-waste-and-recycling/plastics-material-specific-data.
3. Joo, S., et al., *Structural insight into molecular mechanism of poly(ethylene terephthalate) degradation*. Nat Commun, 2018. **9**(1): p. 382.
4. Yoshida, S., et al., *A bacterium that degrades and assimilates poly(ethylene terephthalate)*. Science, 2016. **351**(6278): p. 1196-9.
5. Austin, H.P., et al., *Characterization and engineering of a plastic-degrading aromatic polyesterase*. Proc Natl Acad Sci U S A, 2018. **115**(19): p. E4350-E4357.
6. Wallace, A.C., R.A. Laskowski, and J.M. Thornton, *Derivation of 3D coordinate templates for searching structural databases: application to Ser-His-Asp catalytic triads in the serine proteinases and lipases*. Protein Sci, 1996. **5**(6): p. 1001-13.
7. Glaser, J., A,, *Biological Degradation of Polymers in the Environment*, in *Plastics in the Environment*, Gomiero A, Editor. 2019, IntechOpen.
8. Chen, I.A., et al., *IMG/M v.5.0: an integrated data management and comparative analysis system for microbial genomes and microbiomes*. Nucleic Acids Res, 2019. **47**(D1): p. D666-D677.
9. Taniguchi, I., et al., *Biodegradation of PET: Current Status and Application Aspects*. ACS Catalysis, 2019. **9**(5): p. 4089-4105.
10. Kim, D.E., D. Chivian, and D. Baker, *Protein structure prediction and analysis using the Robetta server*. Nucleic Acids Res, 2004. **32**(Web Server issue): p. W526-31.
11. Trott, O. and A.J. Olson, *AutoDock Vina: improving the speed and accuracy of docking with a new scoring function, efficient optimization, and multithreading*. J Comput Chem, 2010. **31**(2): p. 455-61.
12. Longhi, S., et al., *Atomic resolution (1.0 A) crystal structure of Fusarium solani cutinase: stereochemical analysis*. J Mol Biol, 1997. **268**(4): p. 779-99.
13. Crooks, G.E., et al., *WebLogo: a sequence logo generator*. Genome Res, 2004. **14**(6): p. 1188-90.
14. Altschul, S.F., et al., *Gapped BLAST and PSI-BLAST: a new generation of protein database search programs*. Nucleic Acids Res, 1997. **25**(17): p. 3389-402.
15. UniProt, C., *UniProt: a worldwide hub of protein knowledge*. Nucleic Acids Res, 2019. **47**(D1): p. D506-D515.
16. Jaroszewski, L., et al., *FFAS03: a server for profile--profile sequence alignments*. Nucleic Acids Res, 2005. **33**(Web Server issue): p. W284-8.
17. Ye, Y. and A. Godzik, *Flexible structure alignment by chaining aligned fragment pairs allowing twists*. Bioinformatics, 2003. **19 Suppl 2**: p. ii246-55.
18. Pettersen, E.F., et al., *UCSF Chimera--a visualization system for exploratory research and analysis*. J Comput Chem, 2004. **25**(13): p. 1605-12.
19. Edgar, R.C., *MUSCLE: multiple sequence alignment with high accuracy and high throughput*. Nucleic Acids Res, 2004. **32**(5): p. 1792-7.

20. Trifinopoulos, J., et al., *W-IQ-TREE: a fast online phylogenetic tool for maximum likelihood analysis*. Nucleic Acids Res, 2016. **44**(W1): p. W232-5.
21. Letunic, I. and P. Bork, *Interactive tree of life (iTOL) v3: an online tool for the display and annotation of phylogenetic and other trees.* Nucleic Acids Res, 2016. **44**(W1): p. W242-5.

Figure legends

Figure 1. Binding mode of PET molecule A) Shortened PET molecule 2-HE(MHET)4 docked within the binding site cleft of I. sakaiensis PETase. Surface is colored according to hydrophobicity. B) detailed view of the binding site of I. sakaiensis PETase with docked 2-HE(MHET)4 shortened PET molecule. The catalytic triad residues are colored green, subsite I residues are colored orange, subsite II residues are colored purple, and the disulfide bridge cysteines are colored yellow. This color scheme (consistent with the Joo et. al. 2) will be used throughout the paper to indicate these groups of binding site residues.

Figure 2. The Weblogos of binding site positions of a) metagenomic PETases, b) previously determined PETases and c) cutinases. See Methods section for the description of how the Weblogos were prepared. d) The mapping of Weblogo positions to the sequence numbering of I. sakaiensis PETase. Orange indicates subsite I, violet indicates subsite II, and green indicates catalytic triad. For full sequences, refer to table S3 for previously determined PETases and table S4 for cutinases.

Figure 3. The red stars indicate annotated type I PETases, yellow stars indicate type IIa PETases, and blue stars indicate type IIb PETases (including the I. sakaiensis PETase). The metagenomic sequences are labeled according to their corresponding location and IMG genome ID 1. PETen1 and 2 are labeled by “1” and “2”.

Tables

Table 1. The conservation of functionally important PETase residues in the two most complete putative metagenomic PETase sequences. The top row shows residues and position numbers from *I. sakaiensis* PETase. *I. sakaiensis* PETase residues which are not conserved in metagenomic PETases are colored red. The full sequences of all proposed novel PETases can be found in the supplementary table S2.

Genome / Sample name (link), IMG Genome ID IMG Gene ID (Internal ID)	catalytic triad			subsite I				subsite II					S-S bridge	
	S 160	D 206	H 237	Y 87	Q 119	M 161	W 185	T 88	A 89	W 159	S 238	N 241	C 203	C 239
Desert soil microbial communities from Utah, United States - 20190125_19, 3300036443 Ga0401344_00007_285137_286432 (PETen1)	S	D	H	Y	Q	M	W	L	A	W	S	N	C	C
Vadose zone soil microbial communities from the Eel River Critical Zone Observatory, Northern California, USA - Rivendell_Oct2014_Saprolite_2_DNA_Bulk_2 (SPAdes), 3300027903 Ga0209488_100034395 (PETen2)	S	D	H	F	Q	M	W	T	E	H	S	N	C	C

Table 2. Docking Results The PET molecule used was the shortened tetramer PET molecule 2-HE(MHET)$_4$. The cutin molecule used was linear $C_{24}H_{42}O_8$, an oligo-polyester which mimics some cutin molecules.

	PETen1	PETen2	*I.sakaiensis* PETase	Classical Cutinase (*Fusarium solani pisi*)
Binding Energy (kcal mol^{-1}) - PET	-7.2	-7.3	-7.7	-5.4
Binding Energy (kcal mol^{-1}) - Cutin	-4.0	-3.6	-4.2	-5.8

Figures

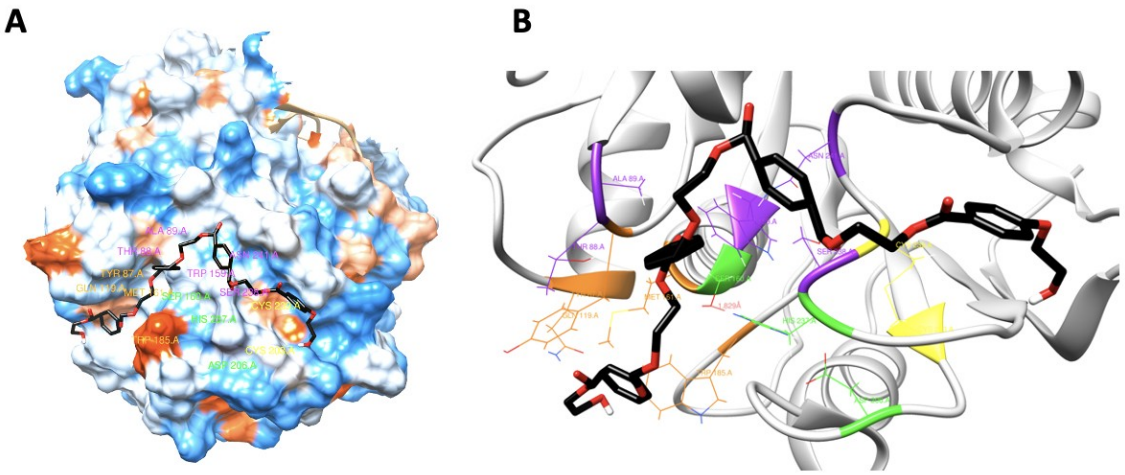

Figure 1.

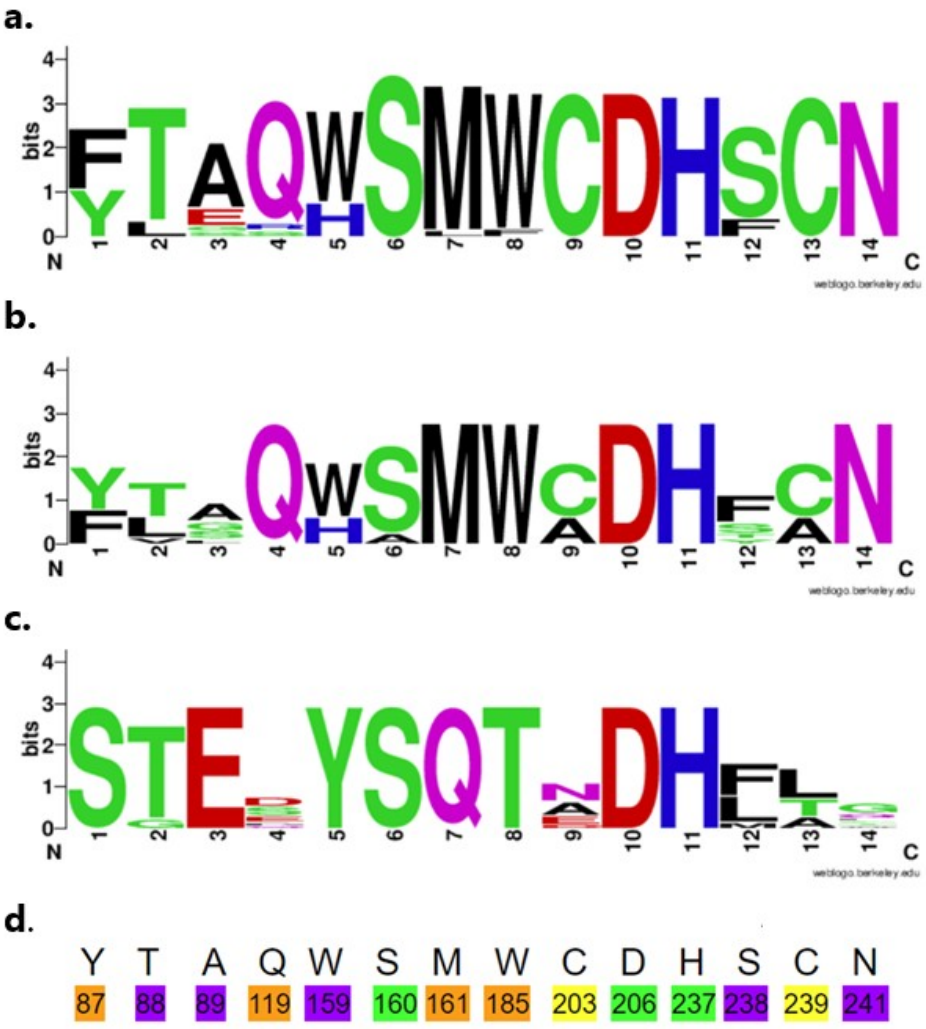
a.
b.
c.
d.
bits
N
C
Y T A Q W S M W C D H S C N
87 88 89 119 159 160 161 185 203 206 237 238 239 241

Figure 2.

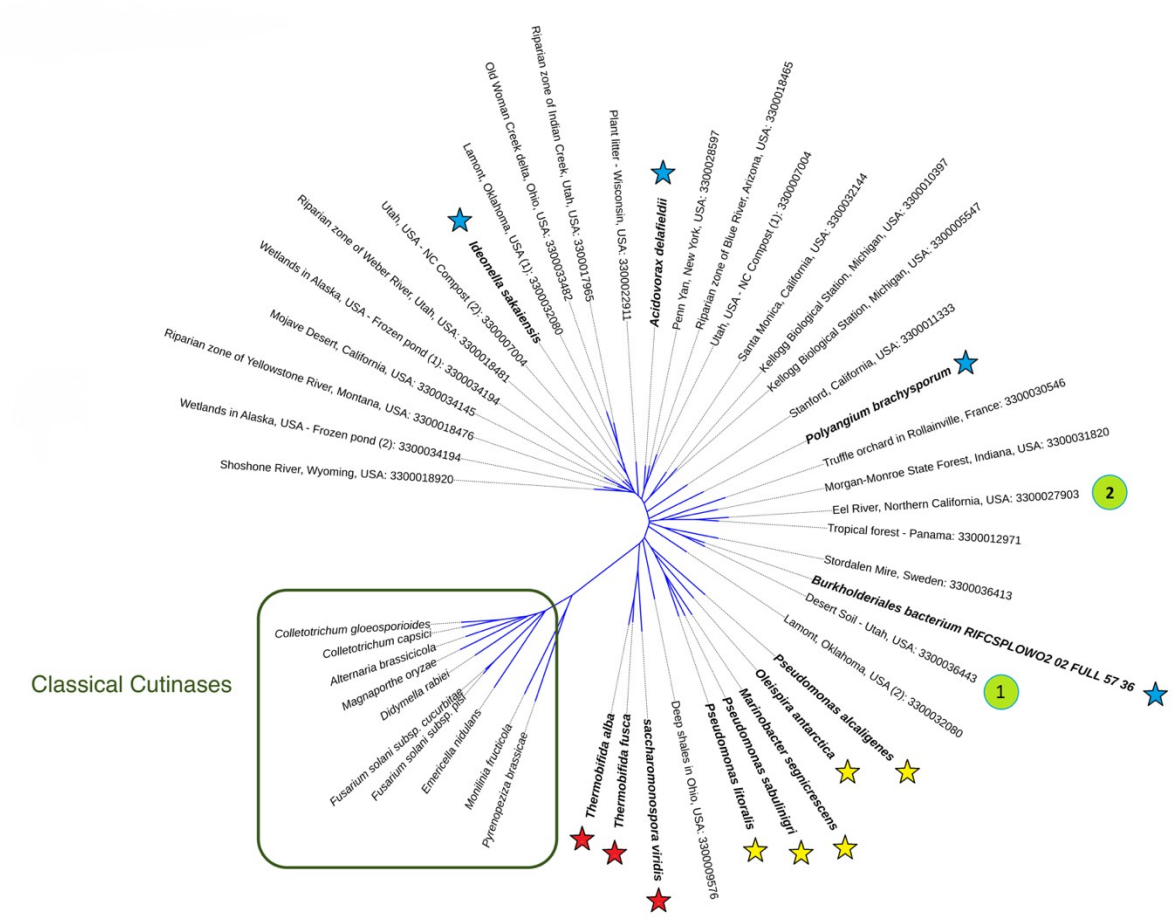
Classical Cutinases
Colletotrichum gloeosporioides
Colletotrichum capsici
Alternaria brassicicola
Magnaporthe oryzae
Didymella rabiei
Fusarium solani subsp. cucurbitae
Fusarium solani subsp. pisi
Emericella nidulans
Monilinia fructicola
Pyrenopeziza brassicae
Thermobifida alba
Thermobifida fusca
saccharomonospora viridis
Deep shales in Ohio, USA: 3300009576
Pseudomonas litoralis
Pseudomonas sabulinigri
Marinobacter segnicrescens
Oleispira antarctica
Pseudomonas alcaligenes
Lamont, Oklahoma, USA (2): 3300032080
Burkholderiales bacterium RIFCSPLOWO2 02 FULL 57 36
Desert Soil - Utah, USA: 3300036443
Stordalen Mire, Sweden: 3300036413
Tropical forest - Panama: 3300012971
Eel River, Northern California, USA: 3300027903
Morgan-Monroe State Forest, Indiana, USA: 3300031820
Truffle orchard in Rollainville, France: 3300030546
Polyangium brachysporum
Stanford, California, USA: 3300011333
Kellogg Biological Station, Michigan, USA: 3300005547
Kellogg Biological Station, Michigan, USA: 3300010397
Santa Monica, California, USA: 3300032144
Utah, USA - NC Compost (1): 3300007004
Riparian zone of Blue River, Arizona, USA: 3300018465
Penn Yan, New York, USA: 3300028597
Acidovorax delafieldii
Plant litter - Wisconsin, USA: 3300022911
Riparian zone of Indian Creek, Utah, USA: 3300017965
Old Woman Creek delta, Ohio, USA: 3300033482
Lamont, Oklahoma, USA (1): 3300032080
Ideonella sakaiensis
Utah, USA - NC Compost (2): 3300007004
Riparian zone of Weber River, Utah, USA: 3300018481
Wetlands in Alaska, USA - Frozen pond (1): 3300034194
Mojave Desert, California, USA: 3300034145
Riparian zone of Yellowstone River, Montana, USA: 3300018476
Wetlands in Alaska, USA - Frozen pond (2): 3300034194
Shoshone River, Wyoming, USA: 3300018920
1
2

Figure 3.